Revealing the Acetylcholinesterase Inhibitory Potential of *Phyllanthus amarus* and Its Phytoconstituents: In Vitro and in Silico Approach

Bioinformatics and Biology Insights
Volume 16: 1–11

DOI: 10.1177/11779322221118330

Kolade O Faloye[1], Shafi Mahmud[2], Emmanuel G Fakola[1], Yemisi M Oyetunde[3], Sunday J Fajobi[4], Jeremiah P Ugwo[5], Ayobami J Olusola[6], Samson O Famuyiwa[1], Oluwabukunmi G Olajubutu[7], Temitope I Oguntade[8] and Ahmad J Obaidullah[9]

[1]Department of Chemistry, Faculty of Science, Obafemi Awolowo University, Ile-Ife, Nigeria. [2]Genetic Engineering and Biotechnology, University of Rajshahi, Rajshahi, Bangladesh. [3]Department of Pharmacognosy, Faculty of Pharmacy, University of Ibadan, Ibadan, Nigeria. [4]Department of Pharmacology, Faculty of Pharmacy, Obafemi Awolowo University, Ile-Ife, Nigeria. [5]Department of Chemistry, School of Science, Federal College of Education, Okene, Okene, Nigeria. [6]Department of Pharmacology, Faculty of Pharmacy, Federal University Oye-Ekiti, Oye-Ekiti, Nigeria. [7]Department of Pharmaceutics, Faculty of Pharmacy, Obafemi Awolowo University, Ile-Ife, Nigeria. [8]Department of Chemical Sciences, Adekunle Ajasin University, Akungba-Akoko, Nigeria. [9]Department of Pharmaceutical Chemistry, College of Pharmacy, King Saud University, Riyadh, Saudi Arabia.

ABSTRACT: The inhibition of acetylcholinesterase plays a vital role in the treatment of Alzheimer disease. This study aimed to explore the acetylcholinesterase inhibition potential of *Phyllanthus amarus* and its phytoconstituents through an in vitro and in silico approach. The in vitro acetylcholinesterase inhibitory activity of *P amarus* was carried out, followed by the molecular docking studies of its phytoconstituents. The top-ranked molecules identified through molecular docking were subjected to molecular dynamics simulation (MDS) and density functional theory (DFT) studies. The results obtained revealed the methanolic extract of *P amarus* as a potent acetylcholinesterase inhibitor, while amarosterol A, hinokinin, β-sitosterol, stigmasterol and ellagic acid were identified as potential acetylcholinesterase inhibitors. The MDS and DFT results are in agreement with those obtained from the docking studies. Our findings suggest further studies on the hit molecules.

KEYWORDS: *Phyllanthus amarus*, acetylcholinesterase, molecular docking, molecular dynamics simulation, density functional theory

RECEIVED: April 1, 2022. **ACCEPTED:** July 18, 2022.

TYPE: Original Research Article

FUNDING: The author(s) received no financial support for the research, authorship and/or publication of this article.

DECLARATION OF CONFLICTING INTERESTS: The author(s) declared no potential conflicts of interest with respect to the research, authorship, and/or publication of this article.

CORRESPONDING AUTHOR: Kolade O Faloye, Department of Chemistry, Faculty of Science, Obafemi Awolowo University, CH112, Ile-Ife, 23401, Nigeria. Email: kollintonx1@gmail.com

Introduction

Alzheimer disease (AD) is a progressive neurodegenerative disorder marked by cognitive and behavioural impairment that significantly interferes with social and occupational functioning. Although a disease of elderly individuals, evidence have shown that younger adults can be affected by AD as early as 40 years of age.[1,2] Currently, more than 55 million people worldwide live with dementia and the number increases by 10 million every year, with AD contributing about 60% to 70%. Hence, AD is the leading cause of dementia.[3]

The AD is a disease condition that comes with episodes of symptoms like memory loss, confusion about familiar location, compromised judgement, loss of spontaneity and mood and personality changes.[4] Although antidepressants, anxiolytics, antiparkinsonian agents, β-blockers and antiepileptic drugs, among others, have been used to treat secondary symptoms associated with AD, the most effective target for AD treatment is the cholinergic transmission.[5] An association has been shown between loss of cholinergic activity and the cognitive weakness in AD. Thus, the inhibition of AChE will result in reversal of deficiency of acetylcholine, which is among the major events in the pathology of AD expressed in the cholinergic hypothesis.[6] Furthermore, the promotion of rapid deposition of β-amyloid by AChE activities can also be prevented by AChE inhibitors, especially those with dual binding capacity.[7]

The standard medical treatments for AD include cholinesterase inhibitors (AChEIs) and a partial N-methyl-D-aspartate (NMDA) antagonist. Donepezil, Galantamine and Rivastigamine (AChEIs) as well as Memantine (NMDA antagonist) are for symptomatic relief and do not treat the underlying cause, nor halt the progression of the disease.[5,8,9] Furthermore, many side effects of these medications and questions on their sustainability as well as lack of response by some patients have led to a search for new drugs, of which herbal medicine is a potential source. In the treatment of diseases, plants have a long history in their use as medicines and as such are important sources of drugs that cannot but be explored in treatment of AD.[10]

Phyllanthus amarus (Euphorbiaceae), also known as black catnip, windbreaker, or carry me seed, is a herb well known for its medicinal properties.[11] The plant belongs to the Phyllanthaceae family, which was previously part of the Euphorbiaceae family and is mostly found in the tropical and subtropical regions of the world, including Africa, Asia, South America and West Indies.[11,12] The whole plant is traditionally used to treat diabetes, jaundice, flu, gonorrhoea, menstrual problem, skin diseases and memory enhancer and dropsy.[11-15] Pharmacologically, its antiviral, anticancer, anti-inflammatory, antioxidant, hypolipidemic, antiplasmodial, antimicrobial and hepatoprotective activities have been reported from various studies.[16-19]

Molecular docking and molecular dynamics simulation have become useful methods of screening huge number of phytochemicals and identifying potential drug candidates.[20-22] Also, density functional theory (DFT) is useful in probing the electronic properties in relation to the pharmacological potentials of phytochemicals.[23]

Despite the evident efficacy of the whole part of *P amarus* as AChE inhibitor,[24] information on the identification of phytoconstituent responsible for its activity is scanty. Therefore, this study aims to validate the AChE inhibitory efficacy of *P amarus* through in vitro evaluation. It further performs the molecular docking studies of phytoconstituents previously isolated from the morphological parts of the plant. Also, molecular dynamics simulation and DFT were performed to elucidate the binding mode and quantum chemical properties of its hit molecules.

Materials and Methods

Plant collection and extraction

P amarus was collected from Obafemi Awolowo University campus, Ile-Ife. Thereafter, it was identified and authenticated by Mr I. I. Ogunlowo of the Faculty of Pharmacy herbarium, Obafemi Awolowo University, Ile-Ife, Nigeria, and its voucher specimen (FPI 2353) was prepared and deposited. Later on, the whole plant was air-dried and pulverized. About 500 g of the powdered plant material was extracted with methanol with occasional shaking for 48 hours. The methanolic solution was filtered and concentrated in vacuo to afford the crude extract (5.2 g).

Receptor and ligand preparation

The 3-dimensional structure of AChE enzyme complexed with dihydrotanshinone I and coded with PDB ID: 4M0E was downloaded from the protein data bank (http://www.rcsb.org/structure/4M0E). The human acetylcholinesterase protein selected for this study consists of 4 chains. The protein's crystal structure was prepared by removing water molecules, native ligand, co-factor, ions and 3 chains (B, C and D). Then, charges and hydrogen were added to the bare protein (chain A) using the MGLTools.

An literature review was conducted to collate the phytoconstituents previously isolated from *P amarus* (see supplementary material).[25-36] The compounds were downloaded from the PubChem database (https://pubchem.ncbi.nlm.nih.gov/) in SDF format, while others were built with Spartan 14 programme. Thereafter, the energy minimization of each ligand was performed under MMFF94x force field using the Open Babel interphase of the PyRx 0.8 software.

Validation of docking protocol and molecular docking studies

The docking protocol used for this study was validated before molecular docking studies were performed on AChE enzyme. In validating the docking protocol, amino acid residues resident with 5 Å in the binding site of the enzyme was chosen (Tyr72, Asp74, Tyr124, Trp286, Ser293, Val294, Phe295, Arg296, Phe297, Tyr337, Phe338 and Tyr341). Thereafter, water molecules, co-factor and native ligand were removed from the binding site of the enzymes. The native ligand removed was re-docked into the binding pocket of the bare protein. The best conformational pose of the re-docked ligand was selected and the root mean square deviation (RMSD) value was computed.

To perform molecular docking, the energy of the phytoconstituents from *P amarus* were minimized under MMFF94x force field using the steepest descent method for 200 steps with a step size of 0.02 and converted from PDB open babel programme in PyRx 0.8 software. Also, the bare proteins were prepared by adding polar hydrogens and merging non-polar hydrogens with MGLTools 1.5.2. Next, the grid box size was set at 40^3 and centre at X = −14.3536, Y = −42.8929, and Z = 24.9102 for the AChE enzyme. Molecular docking was performed to exhaustiveness of 50 using the AutoDock Vina tool in PyRx 0.8.[37] Results obtained with the lowest RMSD value and best binding energy. Later on, interactions like hydrogen bond, hydrophobic and pi were chosen and analysed using Discovery studio visualizer (2020).

Molecular dynamics simulation

The molecular dynamics simulation study was conducted in YASARA dynamics[38] with the aid of the AMBER14 force field.[39] A cubic simulation cell was created with a periodic boundary conditions and TIP3P water solvation model was used.[40] The docked complexes were initially cleaned, optimized and hydrogen bonds were oriented. The simulation cell was extended up to 20 Å at the each case of the complexes. The physiological conditions of the simulations cells were set as 298 K temperature, pH 7.4% and 0.9% NaCl. The long-range electrostatic interactions were calculated by the Particle Mesh Ewald algorithms by a cut-off radius of 8.0 Å.[41-43] The initial energy minimizations of the complexes were done by the steepest gradient algorithms by simulated annealing methods (5000

cycles). The time step of the simulation cell was set as 2.0 fs. The simulation trajectories were saved after every 100 ps.[44] By following constant pressure and Berendsen thermostat, the simulations was extended to 50 ns. The simulations trajectories were used to calculate the RMSD, root mean square fluctuation (RMSF), hydrogen bond, solvent-accessible surface area (SASA) and radius of gyrations.[45-49]

Theoretical modelling and optimization studies

The DFT analysis of the 5 hit molecules from the molecular docking studies with the AChE enzyme was carried out using the Spartan 14 programme containing the functional B3LYP (Lee-Yang Parr exchange-correlation functional method) using a 6-31G basis set.[50] During the calculations, the values of the frontier orbital energies, energy gap, chemical potential, chemical hardness, softness and electrophilicity index were calculated.

In vitro acetylcholinesterase inhibitory assay

The AChE inhibitory activity of the methanolic crude extract of *P amarus* was evaluated by Ellman method[51] as described by Obuotor.[52] The 96-well plates were added with 240 µl of buffer (50 mM Tris-HCl, pH 8.0), 20 µl of varying concentrations (10, 5, 2.5 and 1.25 mg/ml) of the extract dissolved in 5% dimethyl sulphoxide and 20 µl of the enzyme preparation. The reaction mixture was then incubated for 30 min at 37°C, followed by the addition of 20 µl of 10 mM DTNB (5,5' -dithiobis-(2-nitrobenzoic acid)). The reaction was initiated by addition of 20 µl of 25 mM ATChI. The rate of hydrolysis of ATChI was then determined spectrophotometrically by measuring the change in the absorbance per minute (ΔA/min) due to the formation of the yellow 5-thio-2-nitrobenzoate anion at 412 nm over a period of 4 minutes at 30 seconds interval. The buffer solution was used as a negative control. The percentage inhibition (%I) of each sample and the positive control (eserine) were obtained using the formula

$$I(\%) = \left[\frac{(Vo - Vi)}{Vo}\right] \times 100$$

where: I (%) = percentage inhibition, Vi = enzyme activity in the presence of the extract and positive control (eserine) and Vo = enzyme activity in the absence of the extract and positive control (eserine).

Results and Discussion

Analysis of molecular docking studies with acetylcholinesterase enzyme

In validating the docking protocol, co-crystallized and re-docked ligands were aligned and the RMSD value between them was calculated (Figure 1). The RMSD value obtained at 0.01 Å was low and within the acceptable range.

Figure 1. Superimposed image of co-crystallized ligand (green) and re-docked ligand (yellow).

Molecular docking has become a useful method of predicting the bioactive potential of chemical compounds against a target receptor implicated in a disease condition.[53-55] In this study, 5 top-ranked molecules were selected based on their binding energy with the AChE enzyme compared with eserine (–8.2 kcal/mol) (Table 1).

Amarosterol A elicited the best binding energy of –10.0 kcal/mol towards the AChE enzyme. It further established 16 hydrophobic interactions with Tyr124, Phe297, Tyr337, Tyr341 and His441. Also, both pi-sigma and pi-alkyl interactions were formed with Tyr124, Phe297, Tyr337, Tyr341 and His441. However, no hydrogen bonding and electrostatic interactions were established between the AChE enzyme and amarosterol A moiety (Figure 2A).

Hinokinin gave a considerably high binding affinity towards the AChE enzyme at –9.8 kcal/mol. Also, the oxygen atom on the hinokinin moiety participated in 2 hydrogen bond interactions with Tyr124 at 2.3133 Å and Phe295 at 2.4255. The phytochemical further established 3 hydrophobic interactions with Tyr286 andTyr341. Furthermore, 2 pi-alkyl interactions were observed between the hinokinin moiety and Tyr286 and Tyr341 (Figure 2B).

Beta-sitosterol elicited a binding energy of –9.7 kcal/mol at the active site of the AChE enzyme. Six amino acid residues (Tyr124, Trp286, Phe297, Tyr337, Phe338 and Tyr341) participated in 10 hydrophobic interactions with the β-sitosterol moiety. In addition, pi-sigma and pi-alkyl interactions were observed with Tyr124, Trp286, Phe297, Tyr337, Phe338 and Tyr341, while no hydrogen bonding and electrostatic interactions were established between the β-sitosterol moiety and the active site of the AChE enzyme (Figure 2C).

Stigmasterol inhibited the AChE enzyme with a binding energy of –9.5 kcal/mol. It further established 14 hydrophobic interactions with Tyr124, Trp286, Leu289, Val294, Tyr337, Phe338 and Tyr341. Also, both pi-sigma and pi-alkyl interactions were formed with Tyr124, Trp286, Tyr337, Phe338 and Tyr341. However, no hydrogen bonding and electrostatic interactions were established between the AChE enzyme and amarosterol A moiety (Figure 2D).

Table 1. Detailed interaction analysis of top-ranked molecules with AChE enzyme.

LIGAND PUBCHEM ID	BINDING ENERGY (KCAL/MOL)	HYDROGEN BONDING INTERACTION		HYDROPHOBIC INTERACTION	PI INTERACTION
		AMINO ACID RESIDUE	DISTANCE (Å)		
Amarosterol A	–10.0	–	–	Tyr124, Phe297, Tyr337, Tyr341, His441	Tyr124, Phe297, Tyr337, Tyr341, His441
Hinokinin 442879	–9.8	–	–	Trp86, Trp286, Tyr337	Trp86, Trp286, Tyr337
β-sitosterol 222284	–9.6	–	–	Tyr286, Leu289, Phe297, Tyr337, Phe338, Tyr341	Tyr286, Phe297, Tyr337, Phe338, Tyr341
Stigmasterol 5280794	–9.5	–	–	Tyr124, Trp286, Leu289, Val294, Phe297, Tyr337, Phe338, Tyr341	Tyr124, Trp286, Phe297, Tyr337, Phe338, Tyr341
Ellagic acid 5281855	–9.2	Asp74 Tyr124 Phe295	1.9720 2.1989 2.2097	Trp286 Tyr341	Trp286 Tyr341
Eserine	–8.2	Ser293	2.0820	Trp286	Trp286

Abbreviation: AChE, acetylcholinesterase.

Ellagic acid gave binding energy of –9.2 kcal/mol with the AChE enzyme's active site. Three hydrogen bonding interactions (Tyr124 at 2.1989 Å, Phe295 at 2.2097 Å and Tyr74 at 1.9720 Å) were established between 2 oxygen and 1 hydrogen atoms. Furthermore, 9 hydrophobic interactions were formed between Trp286 and Phe341, while pi-pi stacked interactions were established with Trp286 and Phe341. However, no electrostatic interaction was formed with the AChE enzyme (Figure 2E).

The top-ranked phytochemicals and eserine established common hydrophobic and pi interactions with Tyr286. However, only the phytochemicals formed common hydrophobic and pi interactions with Tyr341. Generally, the hydrogen bond, hydrophobic and pi interactions formed between the each phytochemical and the active site of the AChE enzyme account for the unique stability and high binding affinity exhibited by each molecule in the receptor's binding pocket. Hence, the binding energies of the top-ranked phytochemicals are in the order of amarosterol (10.0 kcal/mol) > hinokinin (–9.8 kcal/mol) > β-sitosterol (–9.7 kcal/mol) > stigmasterol (–9.5 kcal/mol) > ellagic acid (–9.2 kcal/mol) > eserine (–8.2 kcal/mol). The results obtained showed that amarosterol A, hinokinin, β-sitosterol, stigmasterol and ellagic acid played a significant role in the acetylcholinesterase activity observed from the methanolic extract of *P amarus*.

Molecular dynamics simulation of top-ranked molecules with AChE enzyme

The molecular dynamics simulation study was conducted to understand the structural variations among the docked complexes across the simulation trajectories. The RMSDs from the C-alpha atoms were assessed to understand the stable nature of the complexes. The RMSD value from the C-alpha atoms from the simulations study demonstrates the degree of flexibility and the mobile nature of the complexes. The higher RMSD related to the more flexible nature, whereas the lower RMSD defines more stable nature of the complexes. Figure 3A indicates that the hinokinin, amarosterol A, β-itosterol, stigmasterol and ellagic acid had initial upper trend and this might be responsible for the flexible nature of the complexes. Therefore, all of the complexes tend to be reached in the steady state after 15 ns times. The β-sitosterol and stigmasterol had comparatively higher trend in RMSD which indicates the relatively flexible nature of this complexes, whereas the hinokinin and amarosterol A had lower RMSD than other complexes. However, all complexes exhibit RMSD lower than 2.5 Å which demonstrates the docked complexes' rigid nature in atomistic simulations.

Moreover, the SASA of the complexes was analysed to understand the changes in the protein surface area where the higher SASA related to the expansion of the surface area and the lower SASA defines the truncated nature of the complexes. Figure 3B indicates that the ellagic acid exhibits relatively higher SASA which demonstrates the extended surface area of the protein complexes upon ligand bindings. The other 4 complexes exhibited a similar trend in SASA and maintained lower degrees of deviations in simulations. The SASA results from the simulations trajectories indicate that the upon binding with the ligand molecules the complexes were stable except ellagic acid.

The radius of gyrations of the complexes was also assessed to understand the mobile nature of the complexes where higher Rg related to the more flexibility while lower Rg related to the strict nature of the complexes. Figure 3C indicates the hinokinin had the lower Rg than other complexes and stigmasterol had the higher Rg; this trend correlates with the RMSD trend of these complexes in simulations. These results demonstrate that the stigmasterol complexes exhibit more flexibility, whereas the hinokinin had more rigid nature.

The hydrogen bond plays an important role in determining the ligand protein interactions in the macromolecular systems. Figure 3D indicates that all complexes had stable hydrogen bond patterning in simulations. Therefore, the RMSFs of the complexes were assessed to explore the flexibility across the amino acid residues of the protein. Figure 3E indicates that maximum residues had RMSF of less than 2.5 Å which defines the stability of the docked complexes. These results indicate that maximum residues from the all complexes exhibit more stable nature.

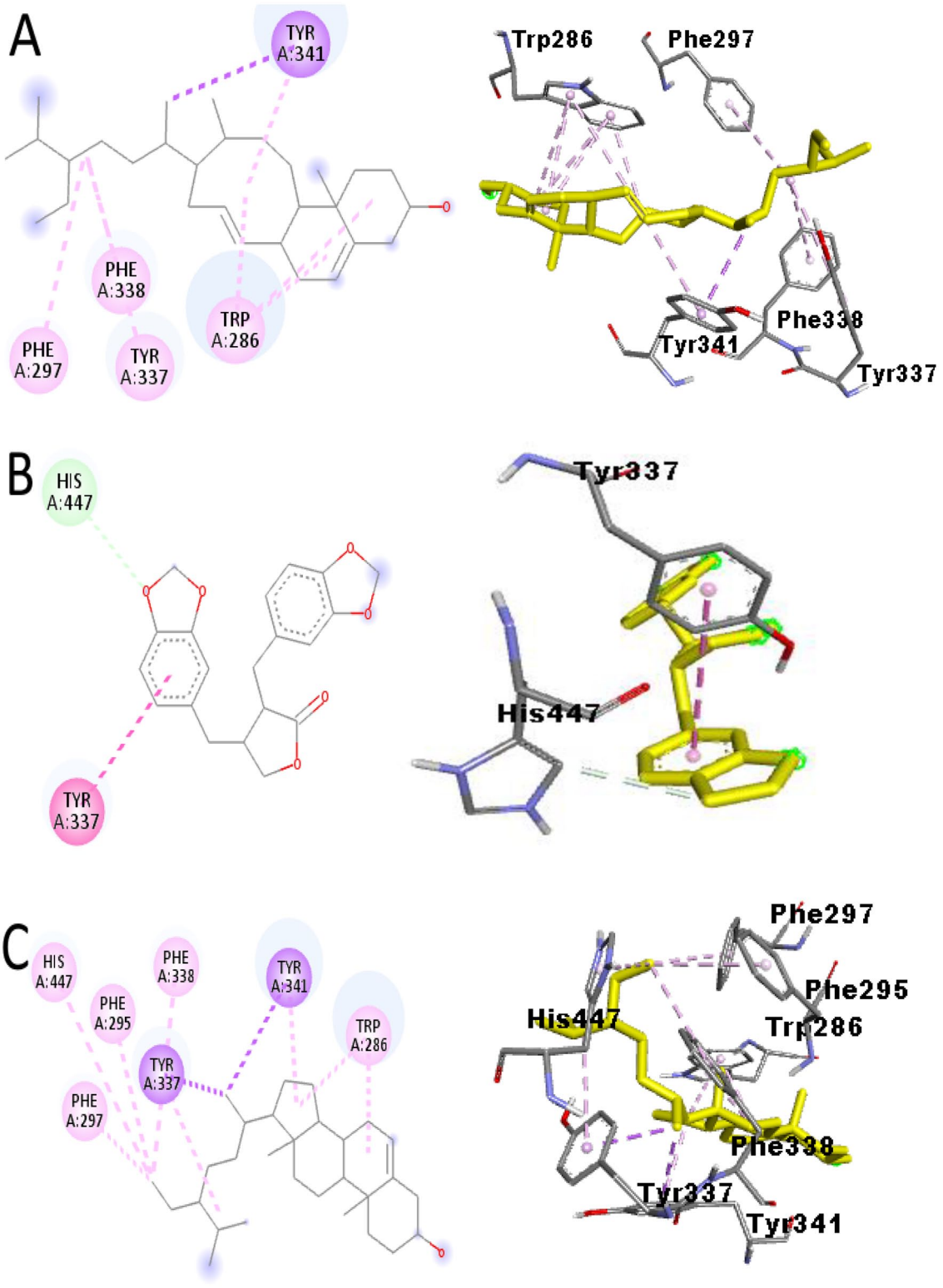

Figure 2. *(Continued)*

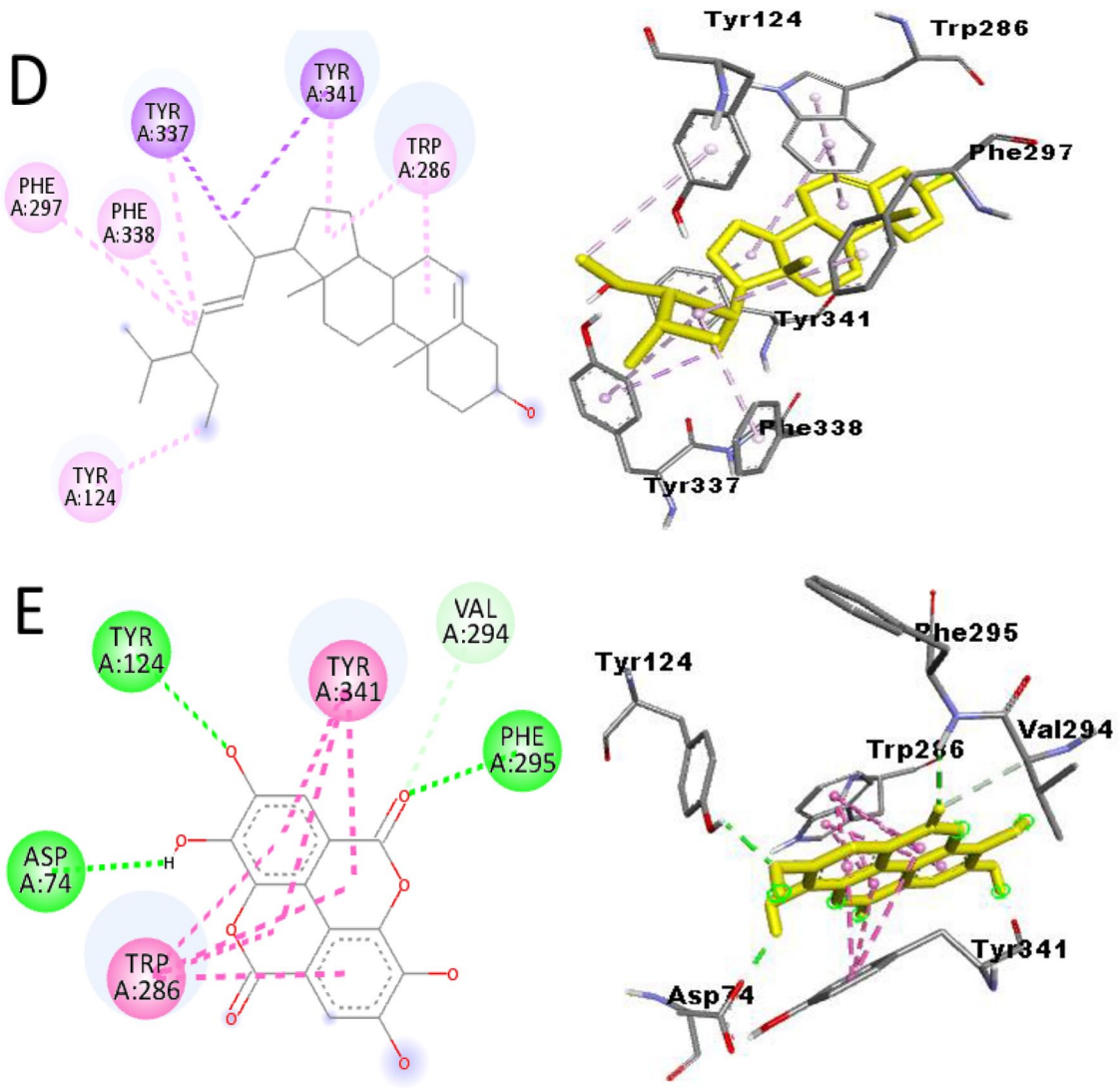

Figure 2. Interaction between amino acid residues in the binding site of AChE and amarosterol A (A), hinokinin (B), β-sitosterol (C), stigmasterol (D) and ellagic acid (E).
AChEI indicates acetylcholinesterase inhibitors.

Frontier molecular orbital and quantum chemical calculation

The highest occupied molecular orbital (HOMO) and lowest unoccupied molecular orbital (LUMO) of molecules are vital parameters that give detailed understanding on the chemical reactivity and stability of chemical constituents. They play important roles in the interactions of the compounds with different enzymes.[56] The HOMO helps to explain the electron-donating potential of the molecule while the LUMO is associated with the electron-accepting ability of the molecule. Therefore, a higher E_{HOMO} value corresponds to a high-donating ability while a low E_{LUMO} value corresponds to a better accepting ability.[57]

The energy gap is a parameter obtained from the E_{HOMO} and E_{LUMO} values and has found wide usefulness in predicting the chemical reactivity of chemical compounds.[58] It is the difference between the E_{LUMO} and E_{HOMO}. Hence, a molecule has high stability and lower reactivity when it has a higher energy gap, while a lower stability and high reactivity corresponds to a low energy gap.[57] Sitosterol elicited the highest energy gap while ellagic acid has the lowest energy gap, thereby suggesting that sitosterol is the most stable molecule and least reactive while ellagic acid is the least stable and most reactive phytochemical. Hence, the calculated energy gap value is in the order of sitosterol > stigmasterol > amarosterol A > hinokinin > ellagic acid (Figures 4 and 5).

To have a vivid understanding of the electronic properties of the phytochemicals, important electronic parameters like chemical potential (μ), chemical hardness (η), softness (S) and electrophilicity index (ω) were calculated (Table 2).

The chemical hardness of a molecule is referred to as the opposition of a molecule to exchange electron density with the environment.[56] A hard molecule is characterized by a large energy gap while soft molecules possess a low energy gap.[57] The energy gap and the hardness of the compounds followed the order ellagic acid < hinokinin < amarosterol A < stigmasterol < sitosterol.

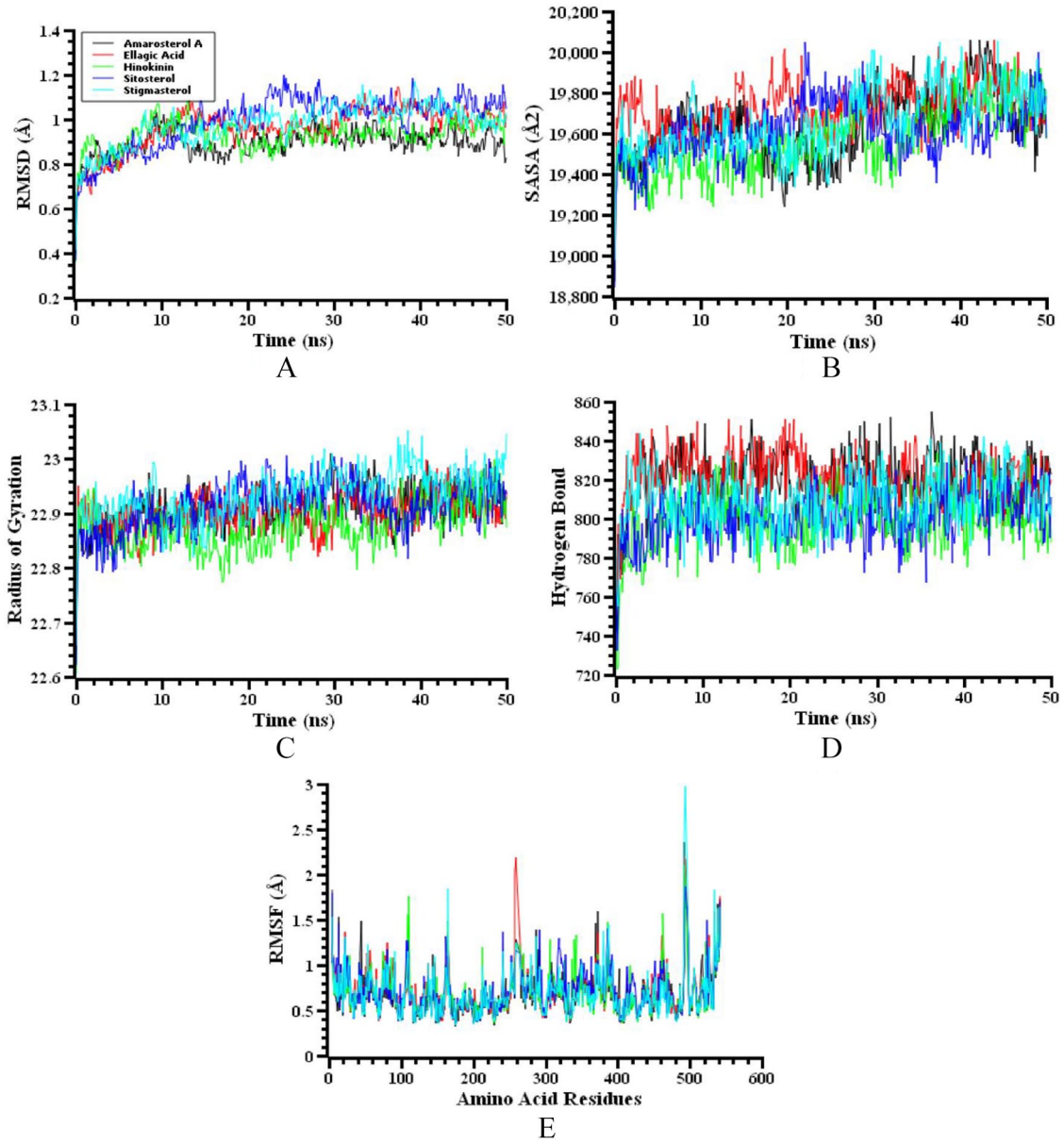

Figure 3. Amarosterol A, hinokinin, β-sitosterol, stigmasterol and ellagic acid with 4M0E; RMSD (A), SASA (B), radius of gyration (C), hydrogen bond (D) and RMSF (E).
RMSD indicates root mean square deviation; RMSF, root mean square fluctuation; SASA, solvent-accessible surface area.

Therefore, sitosterol is the hardest while ellagic acid is the softest (Table 2).

Chemical potential are changes in the energy of a molecule with respect to the electron number at a fixed potential. It elucidates the potential of a chemical compound to exchange electron density with its environment at the ground state and also linked to the electrophilicity index of the molecules.[57,58] Electrophilicity index is a measure of the energy stabilization of a chemical compound as it acquires an extra amount of electronic density from the environment. A strong electrophile possesses a low chemical potential and high chemical hardness, while a weak electrophile possesses high chemical potential and low chemical hardness. Hence, strong electrophiles exhibit high electrophilicity index values while weak electrophiles possess higher lower electrophilicity values.[58-60] Ellagic acid had the highest electrophilicity index while stigmasterol had the lowest. Since the calculated values are more than 0.8, it can be inferred that all the hit molecules had high electrophilicity index values and are likely to act as electrophiles (Table 2).

Molecular electrostatic potential (MESP) is useful in investigating the chemical reactivity of molecules.[60,61] It is a plot of electrostatic potential over constant electron density of molecular systems. The MESP provides a visual representation of the molecular size, shape and potential (positive, negative and neutral) of molecules through a colour grading representation.[23] The molecular electrostatic potential can help in the identification of the reactive sites of electrophilic and nucleophilic

attack in bonding interactions and in the field of biological recognition.[62]

In vitro acetylcholinesterase inhibitory activity of extract of P amarus

The methanolic extract of *P amarus* was tested for its AChE inhibitory potential and compared with eserine (standard drug). The results showed that the extract elicited a considerably high AChE inhibitory activity at $IC_{50}=0.09\pm0.02$ mg/ml compared with eserine at 1.93 ± 0.04 µg/ml. The methanolic extract of *P amarus* showed better AChE inhibitory activity compared with the extracts of *Ipomoea aquatica, Terminalia bellirica* and *Nelumbo nucifera*.[62-64] Polar and non-polar chemical constituents have been identified as potent AChE inhibitors.[65] In our study, the AChE activity elicited by the methanolic extract of *P amarus* can be attributed to the presence of phytochemicals like tannins and terpenoids that are resident in the extract. This can be further substantiated from the binding energy elicited by the terpenoids (amarosterol A, β-sitosterol, stigmasterol and hinokinin) and tannin (ellagic acid).

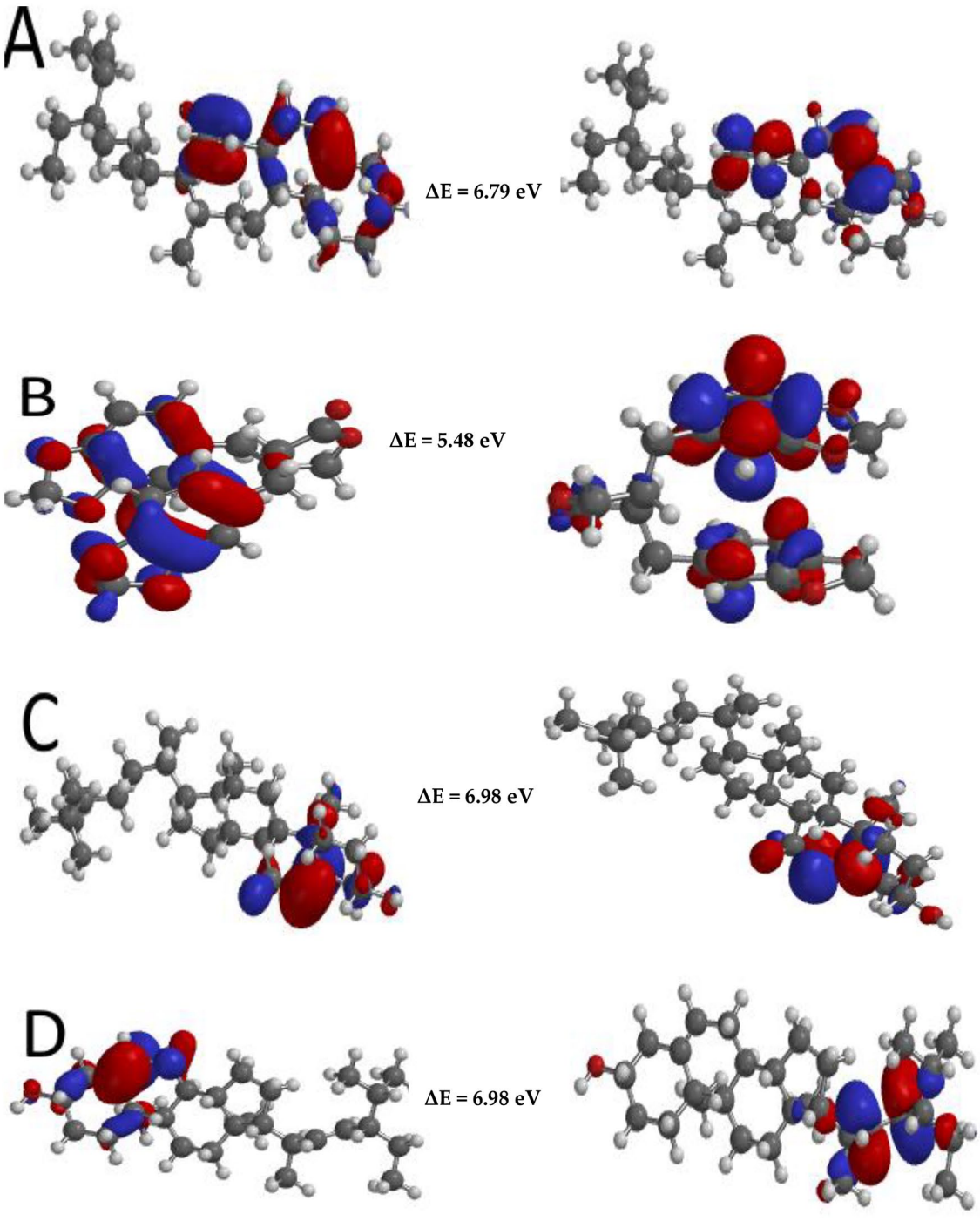

Figure 4. *(Continued)*

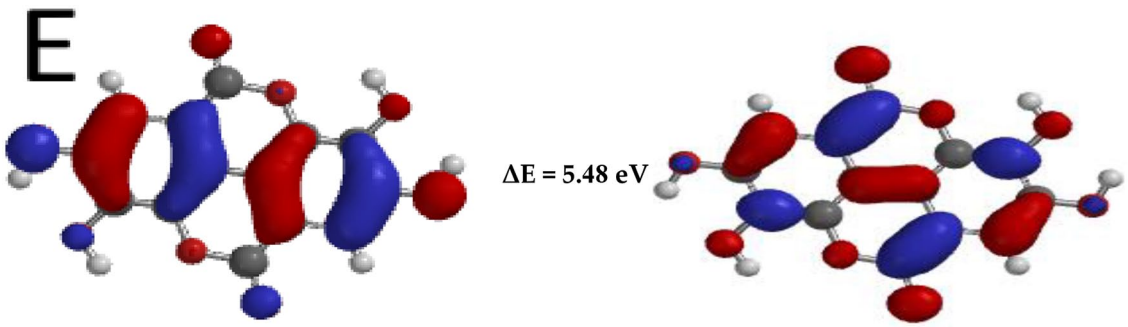

Figure 4. Illustration of the distribution map of the HOMO (A-E), LUMO (unlettered) and the gap energies of amarosterol A (A), hinokinin (B), β-sitosterol (C), stigmasterol (D) and ellagic acid (E).
HOMO indicates highest occupied molecular orbital; LUMO, lowest unoccupied molecular orbital.

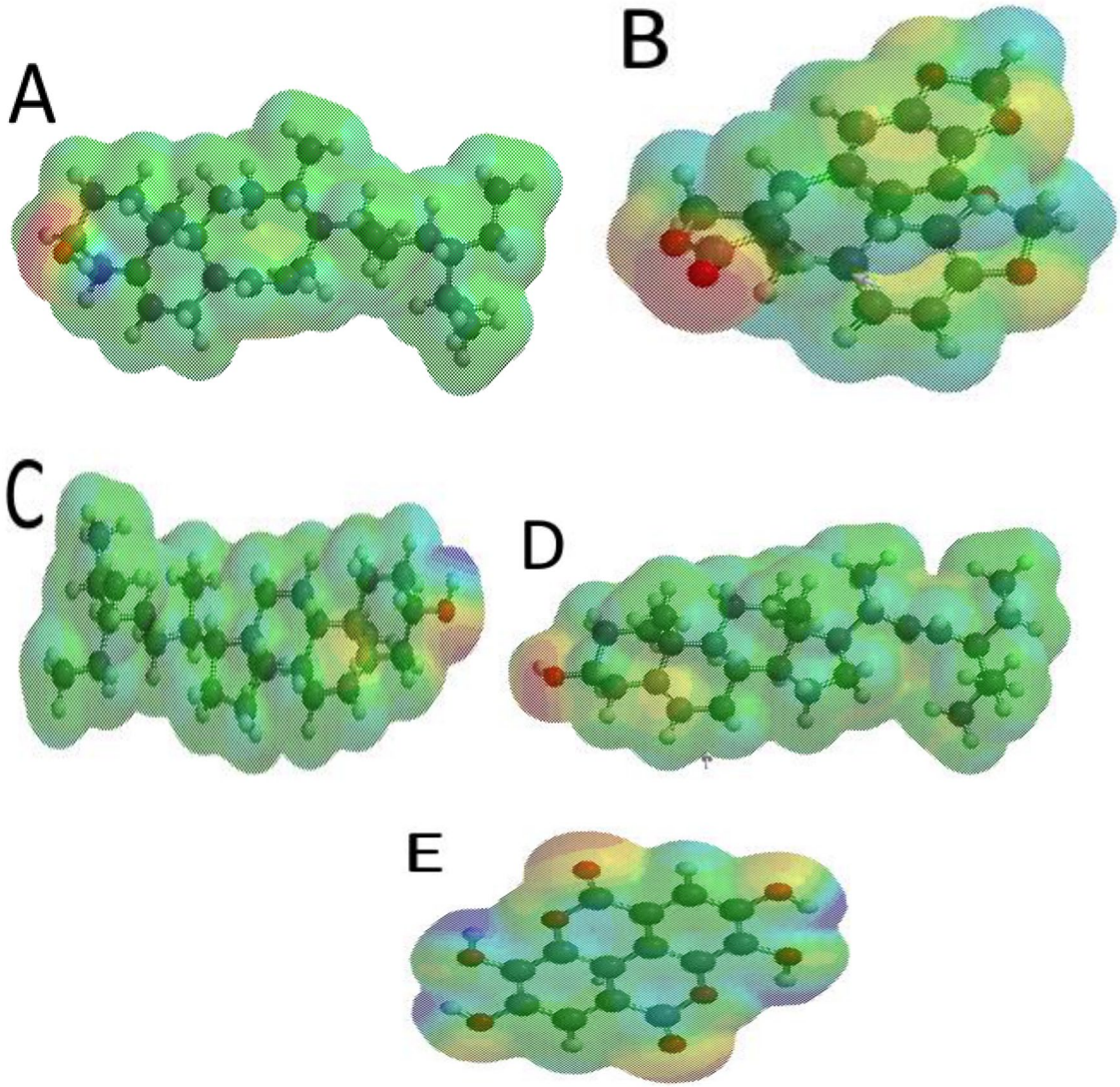

Figure 5. Molecular potential surface of amarosterol A (A), hinokinin (B), β-sitosterol (C), stigmasterol (D) and ellagic acid (E).

Conclusions

This study validated the ethnomedicinal usage of *P amarus* as a memory-enhancing agent. The binding affinity obtained from the molecular docking studies identified compounds in terpenoids and tannin classes as therapeutic agents responsible for the inhibition of AChE. The RMSD and RMSF plots obtained for the top-ranked molecules in the binding pockets of the AChE enzyme showed their stability throughout the entire simulation period. The E_{HOMO}, E_{LUMO}, energy gap and other parameters in the quantum chemical calculations revealed amarosterol A, hinokinin, β-sitosterol, stigmasterol and ellagic acid as promising AChE inhibitors. Hence, the in

Table 2. E_{HOMO}, E_{LUMO} and electronic properties of the chemical compounds.

LIGANDS	E_{HOMO}	E_{LUMO}	ΔE (EV)	η (CHEMICAL HARDNESS)	S (CHEMICAL SOFTNESS)	μ (CHEMICAL POTENTIAL)	ω (ELECTROPHILICITY INDEX)
Amarosterol A	−6.30	0.49	−2.91	3.40	0.29	−2.91	1.24
Hinokinin	−5.68	−0.20	−2.74	2.74	0.36	−2.74	1.37
Sitosterol	−6.14	0.84	−3.49	3.49	0.29	−3.49	1.75
Stigmasterol	−6.15	−0.72	−2.72	3.44	0.29	−2.72	1.07
Ellagic acid	−6.03	−2.04	−4.04	2.00	0.50	−4.04	4.08

Abbreviations: HOMO, highest occupied molecular orbital; LUMO, lowest unoccupied molecular orbital.

silico AChE inhibitory activity of the phytochemicals is in the order of amarosterol A > hinokinin > β-sitosterol > stigmasterol > ellagic acid. The results obtained need to be further validated through in vitro studies to attest to the activity of the compounds.

Author Contributions

Conceptualization, K.O.F and S.O.F; methodology K.O.F, S.M, O.G.O, S.J.F and E.G.F; data analysis, O.G.O, S.J.F and J.P.U; writing – original draft preparation, K.O.F, S.M, Y.M.O and E.G.F; writing – review and editing, S.O.F, K.O.F, S.M, and E.G.F; supervision, K.O.F, S.O.F, Y.M.O and E.G.F; funding acquisition, S.M. All authors have read and agreed to the published version of the manuscript.

Supplemental Material

Supplemental material for this article is available online.

REFERENCES

1. Sugimoto H, Ogura H, Arai Y, Limura Y, Yamanishi Y. Research and development of donepezil hydrochloride, a new type of acetylcholinesterase inhibitor. *Jpn J Pharmacol*. 2002;89:7-20.
2. Joshi H, Parle M. Effects of piperine on memory and behaviour mediated by monoamine neurotransmitters. *J Trad Med*. 2005;23:39-43.
3. World Health Organization. Fact sheets: dementia, https://www.who.int/news-room/fact-sheets/detail/dementia. Assessed October 24, 2021.
4. Akhondzadeh S, Abbasi SH. Herbal medicine in the treatment of Alzheimer's disease. *Am J Alzheimers Dis Other Demen*. 2006;21:113-118.
5. Madhusoodanan S, Shah P, Brenner R, Gupta S. Pharmacological treatment of the psychosis of Alzheimer's disease: what is the best approach? *CNS Drugs*. 2007;21:101-115.
6. Galdeano C, Viayna E, Arroyo E, et al. Structural determinants of the multifunctional profile of dual binding site acetylcholinesterase inhibitors as anti-Alzheimer agents. *Curr Pharm Des*. 2010;16:2818-2836.
7. Potshangbam AM, Nandeibam A, Amom T, et al. An in silico approach to identify potential medicinal plants for treating Alzheimer disease: a case study with acetylcholinesterase. *J Biomol Struct Dyn*. 2022;40:1521-1533. doi:10.1080/07391102.2020.1828170.
8. Winslow BT, Onysko MK, Stob CM, Hazlewood KA. Treatment of Alzheimer disease. *Am Fam Physician*. 2011;83:1403-1412.
9. Massoud F, Leger GC. Pharmacological treatment of Alzheimer disease. *Can J Psychiatry*. 2011;56:579-588.
10. Veeresham C. Natural products derived from plants as a source of drugs. *J Adv Pharm Technol Res*. 2012;3:200-201.
11. Joshi H, Parle M. Pharmacological evidences for anti-amnesic potentials of Phyllanthus amarus in mice. *Afr J Biomed Res*. 2007;10:165-173.
12. Ignacimuthu S, Ayyanar M, Sankarasivaraman K. Ethnobotanical study of medicinal plants used by Paliyar tribals in Theni district of Tamil Nadu, India. *Fitoterapia*. 2008;79:562-568.
13. Shanmugam S, Manikandan K, Rajendran K. Ethnomedicinal survey of medicinal plants used for the treatment of diabetes and jaundice among the villagers of Sivagangai District, Tamil Nadu. *Ethnobot Leafl*. 2009;13:189-194.
14. Samuel JK, Andrews B. Traditional medicinal plant wealth of Pachalur and Periyur hamlets Dindigul District, Tamil Nadu. *Indian J Trad Know*. 2010;9:264-270.
15. Upadhyay B, Parveen AK, Dhaker AK. Ethnomedicinal and ethnopharmaco statistical studies of Eastern Rajasthan, India. *J Ethnopharmacol*. 2010;129:64-86.
16. Lee SH, Jaganath IB, Wang SM, Sekaran SD. Antimetastatic effects of Phyllanthus on human lung (A549) and breast (MCF-7) cancer cell lines. *PLoS ONE*. 2011;6:e20994. doi:10.1371/journal.pone.0020994 2011.
17. Ravikumar YS, Ray U, Nandhitha M, et al. Inhibition of hepatitis C virus replication by herbal extract: Phyllanthus amarus as potent natural source. *Virus Res*. 2011;158:89-97.
18. Guha G, Rajkumar V, Ashok Kumar R, Mathew L. Aqueous extract of Phyllanthus amarus inhibits chromium (VI)-induced toxicity in MDA-MB-435S cells. *Food Chem Toxicol*. 2010;48:396-401.
19. Chirdchupunseree H, Pramyothin P. Protective activity of phyllanthin in ethanol treated primary culture of rat hepatocytes. *J Ethnopharmacol*. 2010;128:172-176.
20. Lokhande KB, Pawar SV, Madkaiker S, Nawani N, Venkateswara SK, Ghosh P. High throughput virtual screening and molecular dynamics simulation analysis of phytomolecules against BfmR of Acinetobacter baumannii: anti-virulent drug development campaign [published online ahead of print February 14, 2022]. *J Biomol Struct Dyn*. doi:10.1080/07391102.2022.2038271.
21. Lokhande KB, Banerjee T, Swamy KV, Ghosh P, Deshpande M. An in silico scientific basis for LL-37 as a therapeutic for Covid-19. *Proteins*. 2022;90:1029-1043.
22. Lokhande KB, Ghosh P, Nagar S, Venkateswara Swamy K. Novel B, C-ring truncated deguelin derivatives reveals as potential inhibitors of cyclin D1 and cyclin E using molecular docking and molecular dynamic simulation. *Mol Divers*. 2022;26:2295-2309.
23. Faloye KO, Bekono BD, Fakola EG, et al. Elucidating the glucokinase activating potentials of naturally occurring prenylated flavonoids: an explicit computational approach. *Molecules*. 2021;26:7211.
24. Feitosa CM, Freitas RM, Luz NN, Bezerra MZ, Trevisan MT. Acetylcholinesterase inhibition by somes promising Brazilian medicinal plants. *Braz J Biol*. 2011;71:783-789.
25. Morton JF. *Atlas of Medicinal Plants of Middle America. Library of Congress Cataloging in Publication Data*. Springfield: Thomas Books; 1981.
26. Sharma A, Singh RT, Anand S. Estimation of phyllanthin and hypophyllanthin by high performance liquid chromatography in Phyllanthus amarus. *Photochem Anal*. 2011;4:226-229.
27. Chevallier A. *Encyclopedia of Herbal Medicine: Natural Health*. 2nd ed. New York: Dorling Kindersley Book; 2000.
28. Srivastava V, Singh M, Malasoni R, et al. Separation and quantification of lignans in Phyllanthus species by a simple chiral densitometric method. *J Sep Sci*. 2008;31:47-55.
29. Kassuya CA, Leite DF, de Melo LV, Rehder VL, Calixto JB. Anti-inflammatory properties of extracts, fractions and lignans isolated from Phyllanthus amarus. *Planta Med*. 2005;71:721-726.
30. Huang RL, Huang YL, Ou JC, Chen CC, Hsu FL, Chang C. Screening of 25 compounds isolated from Phyllanthus species for anti-human hepatitis B virus in vitro. *Phytother Res*. 2003;17:449-453.
31. Singh M, Tiwari N, Shanker K, Verma RK, Gupta AK, Gupta MM. Two new lignans from Phyllanthus amarus. *J Asian Nat Prod Res*. 2009;11:562-568.

32. Maciel MAM, Cunha A, Dantas FTNC, Kaiser CR. NMR characterization of bioactive lignans from Phyllanthus amarus Schum & Thonn. *J Magn Reson Imaging*. 2007;6:76-82.
33. Foo LY, Wong H. Phyllanthusiin D, an unusual hydrolysable tannin from Phyllanthus amarus. *Phytochemistry*. 1993;31:711-713.
34. Foo LY. Amarulone, a novel cyclic hydrolyzable tannin from Phyllanthus amarus. *Nat Prod Lett*. 1993;3:45-52.
35. Londhe JS, Devasagayam TP, Foo LY, Ghaskadbi SS. Antioxidant activity of some polyphenol constituents of the medicinal plant Phyllanthus amarus Linn. *Redox Rep*. 2008;13:199-207.
36. Houghton PJ, Woldemariama TZ, Siobhan OS, Thyagarajan SP. Two securinega type alkaloids from Phyllanthus amarus. *Phytochemistry*. 1996;43:715-717.
37. Trott O, Olson AJ. AutoDock Vina: improving the speed and accuracy of docking with a new scoring function, efficient optimization, and multi-threading. *J Comput Chem*. 2010;31:455-461.
38. Land H, Humble MS. YASARA: A tool to obtain structural guidance in biocatalytic investigations. *Methods Mol Biol*. 2018;1685:43-67. doi:10.1007/978-1-4939-7366-8_4.
39. Wang J, Wolf RM, Caldwell JW, Kollman PA, Case DA. Development and testing of a general Amber force field. *J Comput Chem*. 2004;25:1157-1174. doi:10.1002/jcc.20035.
40. Harrach MF, Drossel B. Structure and dynamics of TIP3P, TIP4P, and TIP5P water near smooth and atomistic walls of different hydroaffinity. *J Chem Phys*. 2014;140:174501.
41. Essmann U, Perera L, Berkowitz ML, Darden T, Lee H, Pedersen LG. A smooth particle mesh Ewald method. *J Chem Phys*. 1995;103:8577-8593. doi:10.1063/1.470117.
42. Harvey MJ, De Fabritiis G. An implementation of the smooth particle mesh Ewald method on GPU hardware. *J Chem Theory Comput*. 2009;5:2371-2377. doi:10.1021/ct900275y.
43. Krieger E, Nielsen JE, Spronk CA, Vriend G. Fast empirical pKa prediction by Ewald summation. *J Mol Graph Model*. 2006;25:481-486. doi:10.1016/j.jmgm.2006.02.009.
44. Krieger E, Vriend G. New ways to boost molecular dynamics simulations. *J Comput Chem*. 2015;36:996-1007. doi:10.1002/jcc.23899.
45. Mahmud S, Biswas S, Kumar Paul G, et al. Antiviral peptides against the main protease of SARS-CoV-2: A molecular docking and dynamics study. *Arab J Chem*. 2021;14:103315. doi:10.1016/j.arabjc.2021.103315.
46. Mahmud S, Biswas S, Paul GK, et al. Plant-based phytochemical screening by targeting main protease of sars-cov-2 to design effective potent inhibitors. *Biology (Basel)*. 2021;10:589. doi:10.3390/biology10070589.
47. Mahmud S, Mita MA, Biswas S, et al. Molecular docking and dynamics study to explore phytochemical ligand molecules against the main protease of SARS-CoV-2 from extensive phytochemical datasets. *Expert Rev Clin Pharmacol*. 2021;14:1305-1315. doi:10.1080/17512433.2021.1959318.
48. Mahmud S, Paul GK, Biswas S, et al. Prospective role of peptide-based antiviral therapy against the main protease of SARS-CoV-2. *Front Mol Biosci*. 2021;8:628585. doi:10.3389/fmolb.2021.628585.
49. Mahmud S, Uddin MAR, Paul GK, et al. Virtual screening and molecular dynamics simulation study of plant-derived compounds to identify potential inhibitors of main protease from SARS-CoV-2. *Brief Bioinform*. 2021;22:1402-1414. doi:10.1093/bib/bbaa428.
50. Becke AD. A new mixing of Hartreee–Fock and local density-functional theories. *J Chem Phys*. 1993;98:1372.
51. Ellman GL, Courtney KD, Andres V Jr, Feather-Stone RM. A new and rapid colorimetric determination of acetylcholinesterase activity. *Biochem Pharmacol*. 1961;7:88-95.
52. Obuotor EM. *The mode of action of Ichthyotoxic principles in Raphia hookeri fruit mesocarp*. PhD Thesis, Obafemi Awolowo University, Ile-Ife, 2004:76-77.
53. Lokhande KB, Apte GR, Shrivastava A, et al. Sensing the interactions between carbohydrate-binding agents and N-linked glycans of SARS-CoV-2 spike glycoprotein using molecular docking and simulation studies. *J Biomol Struct Dyn*. 2022;40:3880-3898.
54. Lokhande KB, Ballav S, Yadav RS, Swamy KV, Basu S. Probing intermolecular interactions and binding stability of kaempferol, quercetin and resveratrol derivatives with PPAR-γ: docking, molecular dynamics and MM/GBSA approach to reveal potent PPAR-γ agonist against cancer. *J Biomol Struct Dyn*. 2020;40:971-981.
55. Lokhande KB, Ballav S, Thosar N, Swamy KV, Basu S. Exploring conformational changes of PPAR-Ɣ complexed with novel kaempferol, quercetin, and resveratrol derivatives to understand binding mode assessment: a small-molecule checkmate to cancer therapy. *J Mol Model*. 2020;26:1-12.
56. Ayeni AO, Akinyele OF, Hosten EC, et al. Synthesis, crystal structure, experimental and theoretical studies of corrosion inhibition of 2-((4-(2-hydroxy-4-methylbenzyl) piperazin-1-yl) methyl)-5-methylphenol–a Mannich base. *J Mol Struct*. 2020;1219:128539.
57. Obi-Egbedi NO, Essien KE, Obot IB, Ebenso EE. 1,2-Diaminoanthraquinone as corrosion inhibitor for mild steel in hydrochloric acid: weight loss and quantum chemical study. *Int J Electrochem Sci*. 2011;6:913-930.
58. Srivastava AK, Pandey AK, Jain S, Misra N. FT-IR spectroscopy, intramolecular C– H···O interactions, HOMO, LUMO, MESP analysis and biological activity of two natural products, triclisine and rufescine: DFT and QTAIM approaches. *Spectrochim Acta A Mol Biomol Spectrosc*. 2015;136:682-689.
59. Domingo LR, Ríos-Gutiérrez M, Pérez P. Applications of the conceptual density functional theory indices to organic chemistry reactivity. *Molecules*. 2016;21:748.
60. Stefaniu A, Pintilie L. *Molecular Descriptors and Properties of Organic Molecules. Symmetry (Group Theory) and Mathematical Treatment in Chemistry*. Rijeka: IntechOpen; 2018:161-176.
61. De Souza TNV, de Carvalho SML, Vieira MGA, da Silva MGC, Brasil DDSB. Adsorption of basic dyes onto activated carbon: experimental and theoretical investigation of chemical reactivity of basic dyes using DFT-based descriptors. *Appl Surf Sci*. 2018;448:662-670.
62. Nwidu LL, Elmorsy E, Thornton J, et al. Anti-acetylcholinesterase activity and antioxidant properties of extracts and fractions of Carpolobia lutea. *Pharm Biol*. 2017;55:1875-1883.
63. Ajayi OS, Aderogba MA, Obuotor EM, Majinda RRT. Acetylcholinesterase inhibitor from Anthocleista vogelii leaf extracts. *J Ethnopharmacol*. 2019;231:503-506.
64. Dhanasekaran S, Perumal P, Palayan M. In-vitro screening for acetylcholinesterase enzyme inhibition potential and antioxidant activity of extracts of Ipomoea aquatica Forsk: therapeutic lead for Alzheimer's disease. *J Appl Pharm Sci*. 2015;5:012-016.
65. Mathew M, Subramanian S. In vitro screening for anti-cholinesterase and antioxidant activity of methanolic extracts of ayurvedic medicinal plants used for cognitive disorders. *PLoS ONE*. 2014;9:e86804.